A response to community questions on the Marine20 radiocarbon age calibration curve: Marine reservoir ages and the calibration of 14C samples from the oceans

Timothy J. Heaton, E Bard, C. Bronk Ramsey, Martin Butzin, Christine Hatté, Konrad A. Hughen, P. Köhler, Paula Jo Reimer

Radiocarbon, Vol 65, Nr 1, 2023, p 247–273 DOI:10.1017/RDC.2022.66

A RESPONSE TO COMMUNITY QUESTIONS ON THE MARINE20 RADIOCARBON AGE CALIBRATION CURVE: MARINE RESERVOIR AGES AND THE CALIBRATION OF ^{14}C SAMPLES FROM THE OCEANS

T J Heaton[1,2*] • E Bard[3] • C Bronk Ramsey[4] • M Butzin[5,6] • C Hatté[7,8] • K A Hughen[9] • P Köhler[5] • P J Reimer[10]

[1]Department of Statistics, School of Mathematics, University of Leeds, Leeds LS2 9JT, UK
[2]School of Mathematics and Statistics, University of Sheffield, Sheffield, S3 7RH, UK
[3]CEREGE, Aix-Marseille University, CNRS, IRD, INRAE, Collège de France, Technopole de l'Arbois BP 80, 13545 Aix en Provence Cedex 4, France
[4]Research Laboratory for Archaeology and the History of Art, University of Oxford, 1 South Parks Road, Oxford OX1 3TG, UK
[5]Alfred-Wegener-Institut Helmholtz-Zentrum für Polar -und Meeresforschung (AWI), D-27515 Bremerhaven, Germany
[6]MARUM–Center for Marine Environmental Sciences, Bremen, Bremen, Germany
[7]Laboratoire des Sciences du Climat et de l'Environnement, CEA, CNRS, UVSQ, Université Paris-Saclay, 91191 Gif-sur-Yvette Cedex, France
[8]Institute of Physics–CSE, Silesian University of Technology, 44-100 Gliwice, Poland
[9]Marine Chemistry and Geochemistry, Woods Hole Oceanographic Institution, Woods Hole, MA 02543, USA
[10]The ^{14}CHRONO Centre for Climate, the Environment and Chronology, Geography, Archaeology and Palaeoecology, Queen's University Belfast BT7 1NN, UK

ABSTRACT. Radiocarbon (^{14}C) concentrations in the oceans are different from those in the atmosphere. Understanding these ocean-atmospheric ^{14}C differences is important both to estimate the calendar ages of samples which obtained their ^{14}C in the marine environment, and to investigate the carbon cycle. The Marine20 radiocarbon age calibration curve is created to address these dual aims by providing a *global-scale* surface ocean record of radiocarbon from 55,000–0 cal yr BP that accounts for the smoothed response of the ocean to variations in atmospheric ^{14}C production rates and factors out the effect of known changes in *global-scale* palaeoclimatic variables. The curve also serves as a baseline to study regional oceanic ^{14}C variation. Marine20 offers substantial improvements over the previous Marine13 curve. In response to community questions, we provide a short intuitive guide, intended for the lay-reader, on the construction and use of the Marine20 calibration curve. We describe the choices behind the making of Marine20, as well as the similarities and differences compared with the earlier Marine calibration curves. We also describe how to use the Marine20 curve for calibration and how to estimate ΔR—the localized variation in the oceanic ^{14}C levels due to regional factors which are not incorporated in the *global-scale* Marine20 curve. To aid understanding, illustrative worked examples are provided.

KEYWORDS: calibration, dating, marine calibration, Marine20, radiocarbon.

1 INTRODUCTION

1.1 Marine Reservoir Ages and the Marine Calibration Curves

In a world unperturbed by anthropogenic emissions, the concentration of ^{14}C in the oceans is always depleted compared with the atmosphere. High frequency variations present in the atmospheric ^{14}C signal are also smoothed out in marine environments. The amount of marine ^{14}C depletion is variable over time, as well as being dependent upon the location and depth of the water. For a specific location and calendar age θ cal yr BP, we quantify the level of ^{14}C depletion using the marine reservoir age (MRA), denoted as $R^{Location}(\theta)$. The MRA defines the difference, at calendar age θ cal yr BP, between the radiocarbon age of dissolved inorganic carbon in the mixed ocean surface layer at that location, and the radiocarbon age of CO_2 in the Northern Hemispheric (NH) atmosphere. Higher MRA

*Corresponding author. Email: t.heaton@leeds.ac.uk

values mean there is a greater level of ^{14}C depletion in the ocean, and a larger disequilibrium with the atmosphere, at that location and time.

There are multiple complex factors affecting the MRA (Bard 1988) but they can be roughly split into those acting at a *global-scale*, and more *localized* effects. The *global-scale* factors include atmospheric CO_2 concentration and ^{14}C production changes, and large-scale changes to ocean circulation and air-sea gas exchange rates. Additional *global-scale* effects include the smoothed and delayed response of the surface oceans, when compared with the more rapid atmospheric response, to variations in ^{14}C production rate which occurs as a consequence of surface waters mixing with the extremely large carbon reservoir in the deeper ocean (Levin and Hesshaimer 2000). The more *local effects*, which would influence the MRA in a smaller neighborhood, might include regional sea-ice, regional winds, water depth, and local upwelling (Key 2001; Reimer and Reimer 2001; Key et al. 2004; Toggweiler et al. 2019). We can therefore partition our location specific, and time dependent, MRA estimate into:

$$R^{Location}(\theta) = R^{GlobalAv}(\theta) + \Delta R^{Location}(\theta),$$

where $R^{GlobalAv}(\theta)$ captures the *global-scale* MRA effects and the oceanic smoothing of high-frequency ^{14}C production rate changes; and $\Delta R^{Location}(\theta)$ the *local* depletion factors (Bard 1988; Stuiver and Braziunas 1993; Heaton et al. 2020).

The goal of the Marine20 calibration curve (Heaton et al. 2020) is to provide a "best estimate" of the *global-scale* surface water ^{14}C concentration in the open ocean that has factored out $R^{GlobalAv}(\theta)$. The Marine20 curve therefore aims to provide a *global-scale* baseline to remove the large-scale effects on the surface ocean MRA of the global palaeoclimatic and carbon cycle variables on which we have current knowledge; and critically also to account for the inherent oceanic smoothing of the high-frequency atmospheric ^{14}C variation.

Oceanic ^{14}C levels vary more smoothly than the atmosphere not only in terms of $\Delta^{14}C$ (vs. calendar age), but also in terms of radiocarbon age (vs. calendar age). Representing this oceanic smoothing of the atmospheric variations in the radiocarbon age over time is one of the primary reasons why a product such as Marine20 is useful for calibration and interpretation of marine ^{14}C samples. To obtain this radiocarbon age smoothing requires careful modeling of the MRA. The value of $R^{GlobalAv}(\theta)$ varies rapidly to account for periods when the atmospheric radiocarbon age has fluctuated in response to a ^{14}C production change, but the ocean's radiocarbon age has not. Such radiocarbon age smoothing cannot be achieved by modeling with a constant MRA, see Section 5.1.1. While a constant MRA (equivalent to a constant proportion of the carbon being ^{14}C-free) will reduce the size of oscillations in the $\Delta^{14}C$ vs. calendar age, in terms of radiocarbon age vs. calendar age it equates to applying a constant offset from the atmospheric equivalent, leaving the size of radiocarbon age vs. calendar age oscillations the same. In this paper, when we discuss the damping of atmospheric signal, we will always be referring to the smoothing of the oscillations in radiocarbon age vs. calendar time unless stated otherwise.

The resultant *global-scale* Marine20 summary is intended to aid the research of two groups of marine ^{14}C users—those archaeologists and environmental scientists wishing to calibrate ^{14}C samples of unknown age that have obtained their carbon from the marine environment; and those palaeoceanographers wishing to understand additional MRA changes and hence finer-scaled behaviour of the carbon cycle and oceans over space and time.

https://doi.org/10.1017/RDC.2022.66 Published online by Cambridge University Press

We stress that all the Marine calibration curves are only intended for the open oceans, in combination with a ΔR atlas. Calibrating ^{14}C samples from closed seas and large lakes, or understanding ^{14}C variation in such locations, is considerably more challenging. We discuss the calibration of such samples in Section 5.1.3.

Notation: Each update of the Marine calibration curve generates new estimates for $R^{GlobalAv}(\theta)$ and consequently will require updates to $\Delta R^{Location}(\theta)$. We now use a subscript to denote the curve-specific values so that, e.g., ${R_{20}}^{GlobalAv}(\theta)$ and $\Delta R_{20}(\theta)$ refer to the *global-scale* and the additional *local-scale* estimates corresponding to the Marine20 curve (Heaton et al. 2020); and ${R_{13}}^{GlobalAv}(\theta)$ and $\Delta R_{13}(\theta)$ the Marine13 values (Reimer et al. 2013). For ease of reading, we drop the location superscript in $\Delta R^{Location}$ where it is not required.

1.2 Intention of this Response to the Community

Following the release of the Marine20 curve (Heaton et al. 2020) we received multiple requests from the ^{14}C community asking if we could provide a more intuitive description of the product aimed at the lay-reader. Motivated by these requests, we have provided this short note.

To guide our response, we collated a set of questions from both archaeological and environmental science users through Dr. Irka Hajdas, Dr. Christine Hatté, and Prof. Tim Jull. These have then been grouped thematically to form the structure of this paper. We split our responses into four sections. Section 2 addresses questions regarding the various uses of Marine calibration curves; and provides a brief summary as to why using Marine20 provides a benefit over Marine13. Section 3 regards the specific construction of the Marine20 curve, and explains the similarities and differences between Marine20 and the earlier Marine calibration curves such as Marine04, 09, and 13 (Hughen et al. 2004b; Reimer et al. 2009, 2013). Section 4 concentrates on the implications for users and provides worked examples of how to estimate $\Delta R(\theta)$ for a particular location using the Marine20 curve and how to then calibrate ^{14}C determinations. It is key to understand that these $\Delta R(\theta)$ values must be updated to $\Delta R_{20}(\theta)$ when using the Marine20 calibration curve. Finally in Section 5, we address further miscellaneous questions on the use of Marine20 which the community have raised.

Some of our responses overlap with information given in the Marine20 paper (Heaton et al. 2020). However, here we have tried to provide a more intuitive understanding—minimizing technical detail but keeping the essential ideas. We hope this approach is more accessible for the highly diverse range of potential Marine20 users. Those readers seeking greater modeling details should refer to Heaton et al. (2020).

2 WHAT IS MARINE20 FOR? WHY IS IT AN IMPROVEMENT OVER MARINE13?

2.1 Uses of Marine20

Broadly speaking, Marine20 has two groups of users: those who have known-age marine ^{14}C samples who want to understand variations in oceanic ^{14}C depletion and hence investigate potential changes to the carbon cycle; and those seeking to calibrate marine ^{14}C samples. The needs of these two user groups are strongly linked.

https://doi.org/10.1017/RDC.2022.66 Published online by Cambridge University Press

2.1.1 To study MRA changes beyond those caused by oceanic smoothing of atmospheric ^{14}C and global palaeoclimatic variables

Palaeoceanographers are typically interested in understanding the spatial and temporal variations in MRA using ^{14}C determinations for which they also have independent calendar age estimates. Estimates of region-specific MRA variations that enable insight into potential carbon cycle changes can be most usefully obtained by considering the offset between the Marine20 curve and their ^{14}C data. This offset is $\Delta R_{20}(\theta)$.

The ocean and the atmosphere respond differently to variation in ^{14}C production rates. Changes in atmospheric ^{14}C levels typically take time to be transferred to the surface ocean and are also significantly damped (Druffel and Suess 1983; Grottoli and Eakin 2007; Komugabe-Dixson et al. 2016; Bard and Heaton 2021). This is a consequence of mixing between the surface layer of the ocean and the extremely large carbon reservoir in deeper ocean layers (in total, during late-Holocene/pre-industrial times, the ocean contained ~ 60 times more carbon than the atmosphere), and the slow rate of air-sea CO_2 equilibration (Grottoli and Eakin 2007; Skinner and Bard 2022). The resultant smoothing, and phase shift, of changes in atmospheric ^{14}C levels that is inherent to the surface ocean causes considerable high-frequency variation in the overall MRA at any site—whereby atmospheric ^{14}C levels have changed but the ocean is still in the process of responding/equilibrating—see Figure 1 for a model-based illustration of the effect on overall MRA of this ocean smoothing.

These high-frequency changes in overall MRA, that occur solely due to oceanic smoothing of atmospheric ^{14}C production, are not however of primary interest for those aiming to understanding carbon cycle changes. In fact, they are typically nuisance variables that act as confounders, hindering useful inference about carbon cycle changes when comparing observed ^{14}C samples across oceanic sites or over time. Ideally, we would wish to remove, or factor out, these smoothing-based (nuisance) variations in overall MRA so that we can study and discover other, more scientifically interesting, causes for changes in oceanic ^{14}C depletion levels more easily.

Equally, we would wish to factor out those confounding changes in overall MRA that are due to changes in *global-scale* palaeoclimate variables, for example those due to variations in CO_2 concentration (Köhler et al. 2017), wind speed (Petit et al. 1990; McGee et al. 2010; Kohfeld et al. 2013; Kageyama et al. 2021), or in the Atlantic meridional overturning circulation (AMOC) (Böhm et al. 2015; Henry et al. 2016; Oka et al. 2021) and wider carbon cycle (Bauska et al. 2021). Factoring out the effect of these variables allows us to better compare changes in the carbon cycle over time between different oceanic locations, especially when we do not have contemporaneous ^{14}C samples from all our sites. After having factored out the effect of *global-scale* variables, if we can identify that further MRA changes have occurred in one location, but not another, then this suggests localized carbon cycle variations.

Given known-age marine ^{14}C samples from a specific location, both the inherent oceanic smoothing and *global-scale* confounders in overall MRA can be factored out by studying $\Delta R_{20}(\theta)$, the offset of the specific samples to the Marine20 curve. Marine20 accounts for the damping of fine-scale atmospheric ^{14}C variation which occurs in the oceans, and also incorporates the *global-scale* MRA effects. Consequently, studying the $\Delta R_{20}(\theta)$ offset allows the disentangling of any confounding MRA changes that are due to global palaeoclimatic variables and the oceanic smoothing of rapid atmospheric ^{14}C changes. Changes in $\Delta R_{20}(\theta)$

https://doi.org/10.1017/RDC.2022.66 Published online by Cambridge University Press

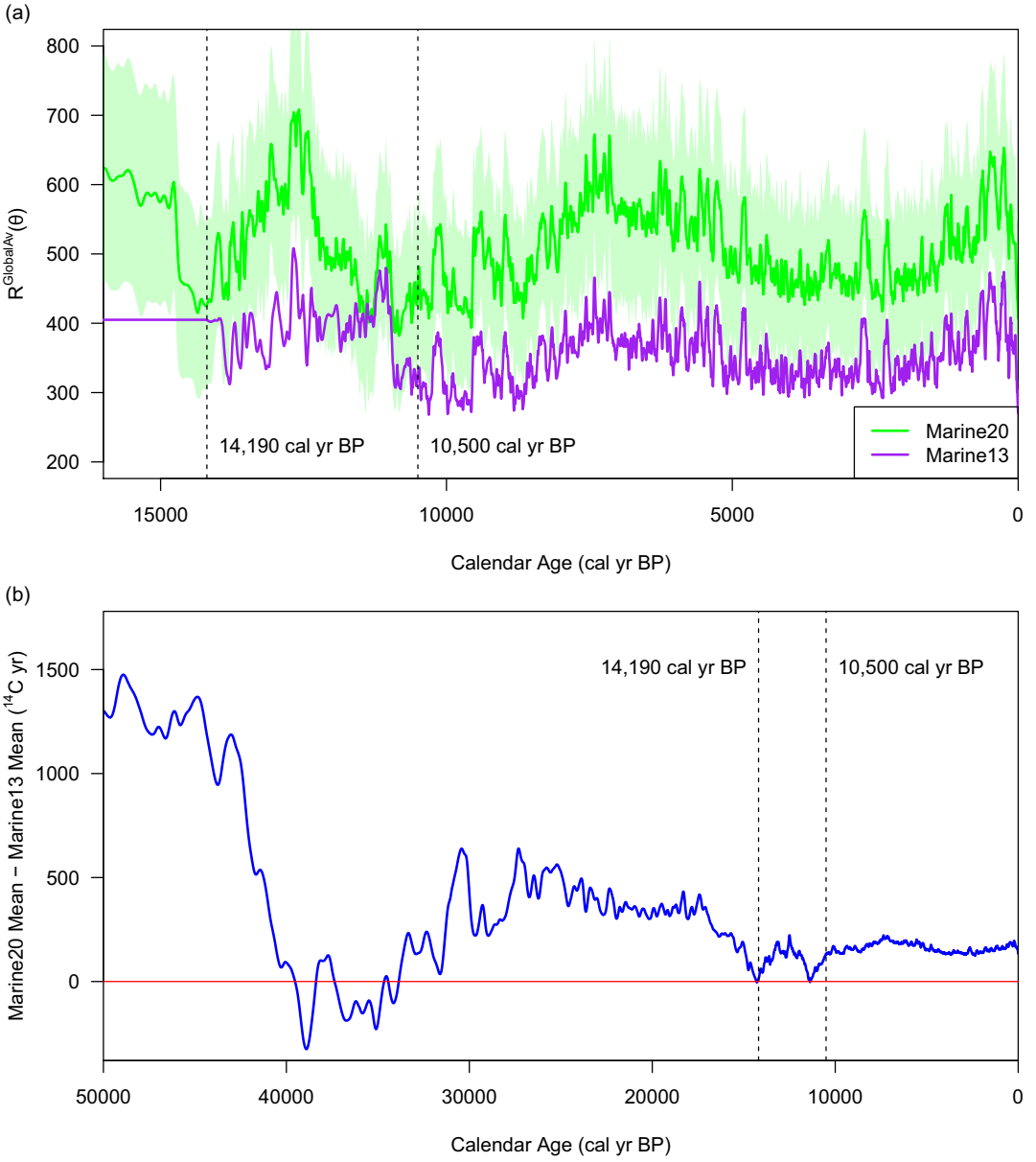

Figure 1 Panel (a) The mean $R_{20}^{GlobalAv}(\theta)$ estimate of Marine20 (green, shown with 2σ-intervals) vs. the mean $R_{13}^{GlobalAv}(\theta)$ of Marine13 (purple) from 15,000–0 cal yr BP. The vertical lines (at 14,190 and 10,500 cal yr BP) denote the breakpoints between the three different methods employed to construct the Marine13 curve. These plotted curves should be thought of as providing estimates for global-scale changes in MRA over time rather than a specific "global-average" MRA. Since the overall ^{14}C depletion in any specific location is offset from these values by ΔR, it is the shape of $R^{GlobalAv}(\theta)$ which is important for inference rather than their absolute values. From 10,500–0 cal yr BP, the shape of $R_{20}^{GlobalAv}(\theta)$ remains similar to $R_{13}^{GlobalAv}(\theta)$ indicating estimates of global-scale MRA changes and the overall estimates of ^{14}C depletion at a specific oceanic site do not change substantially with Marine20 in this period. Further back in time, estimated changes in depletion are however significant. Panel (b) The offset between the mean of the Marine20 curve and the Marine13 curve. From 10,500–0 cal yr BP, the offset remains approximately constant over time as, during this time period, neither the atmospheric ^{14}C estimate (IntCal13 vs. IntCal20) nor the global-scale effects ($R_{13}^{GlobalAv}(\theta)$ vs. $R_{20}^{GlobalAv}(\theta)$) diverge. Further back in time, from 55,000–10,500 cal yr BP the differences between Marine20 and Marine13 are due to the combination of improvements in the modeling of $R_{20}^{GlobalAv}(\theta)$ and improved knowledge of atmospheric ^{14}C levels available in IntCal20.

https://doi.org/10.1017/RDC.2022.66 Published online by Cambridge University Press

over both space and time can therefore help to inform on important changes in localized oceanic conditions.

This approach to understanding variations in the carbon cycle, in particular those concerning ocean circulation and ventilation, by estimating changes in $\Delta R(\theta)$ has been employed in multiple marine locations. Examples include the Southern Ocean (van Beek et al. 2002); the Atlantic Ocean (Waelbroeck et al. 2019); tropical Atlantic (Hughen et al. 2004a); the North Atlantic and Norwegian Seas (Bondevik et al. 2006; Ascough et al. 2009; Muschitiello et al. 2019; Brendryen et al. 2020); the Gulf of Oman (Lindauer et al. 2017); and the Florida Keys reef tract (Toth et al. 2017). Research has also been undertaken to understand $\Delta R(\theta)$ variability, and its potential causes, in a range of Pacific Ocean locations including the Gulf of Panamá (Toth et al. 2015); off the coast of Peru and Chile (Ortlieb et al. 2011; Carré et al. 2016; Latorre et al. 2017); the South China Sea (Yu et al. 2010; Hirabayashi et al. 2019; Hua et al. 2020); and the South Pacific, including the central South Pacific Gyre (Petchey 2020), New Zealand (Petchey and Schmid 2020), Papua New Guinea (McGregor et al. 2008), Vanuatu and the Solomon Islands (Burr et al. 2015), the Great Barrier Reef (Hua et al. 2015, 2020), and the South Tasman Sea (Komugabe-Dixson et al. 2016). In some locations, changes over time in the observed value of $\Delta R(\theta)$ appear to be relatively small, while in other regions larger temporal variations are seen. Readers should note that the estimates of changes in $\Delta R(\theta)$ over time in these papers relate to previous versions of the Marine calibration curve. They will need updating in light of the improved Marine20—although we expect that inference on variations in $\Delta R(\theta)$ in the Holocene will remain similar due to the relatively limited changes in the Marine13 and Marine20 estimates (beyond a constant offset) in this time period.

We also note that the global-scale estimates of MRA, ${R_{20}}^{GlobalAv}(\theta)$, that are produced by Marine20 are also useful for those using directly-paired atmospheric and marine ^{14}C samples to estimate variations in overall MRA (e.g., Bard et al. 1994; Siani et al. 2001, 2013; Skinner et al. 2017; Telesiński et al. 2021). These studies, looking at direct ocean-atmospheric ^{14}C age differences $R^{Location}(\theta)$, are somewhat hampered when seeking to infer which changes are due to variations in CO_2 levels or ^{14}C production rates; and which are due to localized ocean ventilation changes. Separating out these effects can be improved by comparing the overall changes they observe in $R^{Location}(\theta)$ to our Marine20 estimate of ${R_{20}}^{GlobalAv}(\theta)$.

2.1.2 To calibrate new marine ^{14}C samples

Those seeking to calibrate new marine ^{14}C determinations from a specific location need a local marine ^{14}C calibration curve. Currently, we have insufficient knowledge about the local factors affecting MRA to accurately model region-specific calibration curves. For most locations, we also cannot obtain good data-based estimates of $\Delta R(\theta)$ over prolonged periods—which could otherwise be used to create a local marine calibration curve—due to a sparsity of ^{14}C data for which calendar ages are independently known (see Section 2.1.3 for more details on regional calibration curves).

If we wish to calibrate marine ^{14}C samples from a particular location, we are therefore required to make a significant simplification. This simplification, used since the first Marine calibration curve (Stuiver et al. 1986), is to model the localized $\Delta R(\theta)$ in the location of interest as being approximately constant, or at most to vary relatively slowly, over time. This simplification permits us to obtain an estimate for a local marine calibration curve using Marine20 in

https://doi.org/10.1017/RDC.2022.66 Published online by Cambridge University Press

combination with known-age ^{14}C samples, or paired marine and terrestrial ^{14}C samples, from the site of interest.

We recognize that this simplification is a very significant approximation and lies at odds with Section 2.1.1. In practice, we should expect $\Delta R(\theta)$ to vary over time in any location due to changes in local ocean circulation or other localized factors. The scale of these $\Delta R(\theta)$ changes over time will vary dependent upon the location, as shown by the various research in Section 2.1.1. In certain locations, variation over time will be small and so the approximation will be good; in others there may have been larger changes in $\Delta R(\theta)$ over time and treating it as approximately constant will be a much coarser approximation. However, such a simplification does permit the user ^{14}C community to implement a standardised approach to marine calibration that can be used until our knowledge improves and reliable regional marine calibration curves become available. If possible, we always recommend users try and use an estimate of $\Delta R(\theta)$ from a calendar age that is as close to the age of their specific samples as possible to limit the impact of potential $\Delta R(\theta)$ changes.

If we are willing to assume that, in our ocean location of interest, the additional local depletion effects $\Delta R(\theta)$ are approximately constant over time, then we can use known-age ^{14}C data from that location to estimate a constant ΔR. In the case of Marine20 this is denoted ΔR_{20}. Such a ΔR_{20} can then be used to adjust Marine20 and provide a localized calibration curve. Ideally, one would obtain this estimate of ΔR_{20} based on ^{14}C samples of similar calendar age to that which one is calibrating—for example, if one has an archaeological site with tightly linked (contemporaneous) shells and charcoal, or paired U-Th and ^{14}C dates on the same ocean coral. However, if it is not possible to obtain an estimate of ΔR_{20} using data of a similar calendar age to that one wishes to calibrate, one must rely upon ^{14}C data from the recent past. A maintained database to enable estimation of regional ΔR_{20} based on such recent samples is provided at http://calib.org/marine/ (Reimer and Reimer 2001).

During the Holocene, to enable ^{14}C calibration, a simplification of an approximately constant $\Delta R(\theta)$ over time is perhaps justifiable for a broader range of ocean locations due to the relatively stable global climate. However, for samples that come from before the onset of the Holocene, such a simplification certainly cannot be justified at higher latitudes (outside ca. 40°S–40°N). During glacial periods, these high latitude regions may have seen localized sea-ice cover, strong winds, and ocean circulation changes that could have had very significant additional short-term effects on $\Delta R(\theta)$ (Butzin et al. 2005; Völker and Köhler 2013). Consequently, in these polar regions, the assumption of a constant $\Delta R(\theta)$ extending into glacial stadials is inappropriate (Butzin et al. 2017). We do not recommend the use of Marine20, with a constant ΔR_{20} estimated from Holocene samples, to calibrate ^{14}C samples from polar regions (outside ca. 40°S–40°N) that are older than ca. 11.5 cal kyr BP.

This latitudinal polar divide (of 40°S–40°N) is based on the geometry of low- versus high-latitudinal areas in the BICYCLE model. Simulations with the three-dimensional LSG ocean general circulation model suggest that temporal changes in the presence of sea ice may have the largest influence on ΔR. In regions where sea ice formation can be excluded, Marine20 might still be applicable outside the stated low-latitudinal core area, but should be done so with great caution. We also do not provide an exact date as to when significant changes in $\Delta R(\theta)$ are likely to have occurred in polar regions. These decisions should be

https://doi.org/10.1017/RDC.2022.66 Published online by Cambridge University Press

made and justified by the calibration user, drawing on various lines of palaeoclimatic or proxy evidence on the extent of localized sea-ice they may have.

Crucially, this caution regarding the unsuitability for polar calibration in glacial periods is equally valid, if not more so, for any of the earlier Marine calibration curves provided by the IntCal group (e.g., Hughen et al. 2004b; Reimer et al. 2009, 2013). The use of Marine20, or any of the earlier Marine calibration curves, using a constant (Holocene-based) ΔR is likely to significantly underestimate the calendar age uncertainty of glacial-period polar oceanic ^{14}C samples and introduce biases, providing calendar age estimates that may be substantially older than the true age of the ^{14}C sample. See Section 2.1.6 and Heaton et al. (2022) for further advice on calibration of polar marine ^{14}C samples.

2.1.3 Calibration using data-based regional marine calibration curves

As explained above, in all marine locations, the value of $\Delta R(\theta)$ will, to a greater or lesser extent, change over time. All users should therefore be aware of the current limitations of using a constant-adjusted Marine20 (or any earlier Marine curve) when calibrating marine ^{14}C samples and should treat their calendar age estimates with caution accordingly, especially in marine regions where they think local hydrographic conditions will have changed significantly.

The range of recent research, described in Section 2.1.1, that uses ^{14}C samples to provide insight into the scale of changes to $\Delta R(\theta)$ over time has the potential to enable the creation of regional, data-based, marine calibration curves in some selected locations. Production of such regional curves is however extremely challenging due to the typical sparsity of available ^{14}C marine samples over long time periods, as well as the difficulty in obtaining independent calendar age estimates for them. This is particularly an issue if we wish to create calibration curves which extend far into our past. There are also significant unanswered questions regarding the area over which such observational ^{14}C marine data might reasonably be combined into a single regional curve, and similarly the extent of the spatial neighborhood in which any consequent regional marine curve might be applicable for calibration.

Examples of research on changes in $\Delta R(\theta)$ where, due to the volume of ^{14}C data from the region that is available, individuals have begun to propose and create regional data-based marine calibration curves covering more prolonged periods include the North Atlantic (Skinner et al. 2019; Waelbroeck et al. 2019), the Norwegian Sea (Muschitiello et al. 2019), and South Florida (Toth et al. 2017). In the Pacific, there is also the Gulf of Panamá (Toth et al. 2015), New Zealand (Petchey and Schmid 2020), the Great Barrier Reef and the South China Sea (Hua et al. 2020).

We do not feel able to endorse specific regional calibration curve products but we note that, for some ^{14}C users, these regional marine curves may be appropriate for calibration. As our knowledge and data improve, we expect that more reliable, and more precise, regional calibration curves will become available. However, where $\Delta R(\theta)$ is unknown, approximations and simplifications are currently still required for most ^{14}C users.

2.2 Why is Marine20 an Improvement over Marine13?

Most simply, Marine20 aims to offer a substantial improvement in the modeling and estimation of the *global-scale* ^{14}C depletion effects [i.e., ${R_{20}}^{GlobalAv}(\theta)$] compared to the ${R_{13}}^{GlobalAv}(\theta)$ estimate used in Marine13. This is achieved by transient application of the

https://doi.org/10.1017/RDC.2022.66 Published online by Cambridge University Press

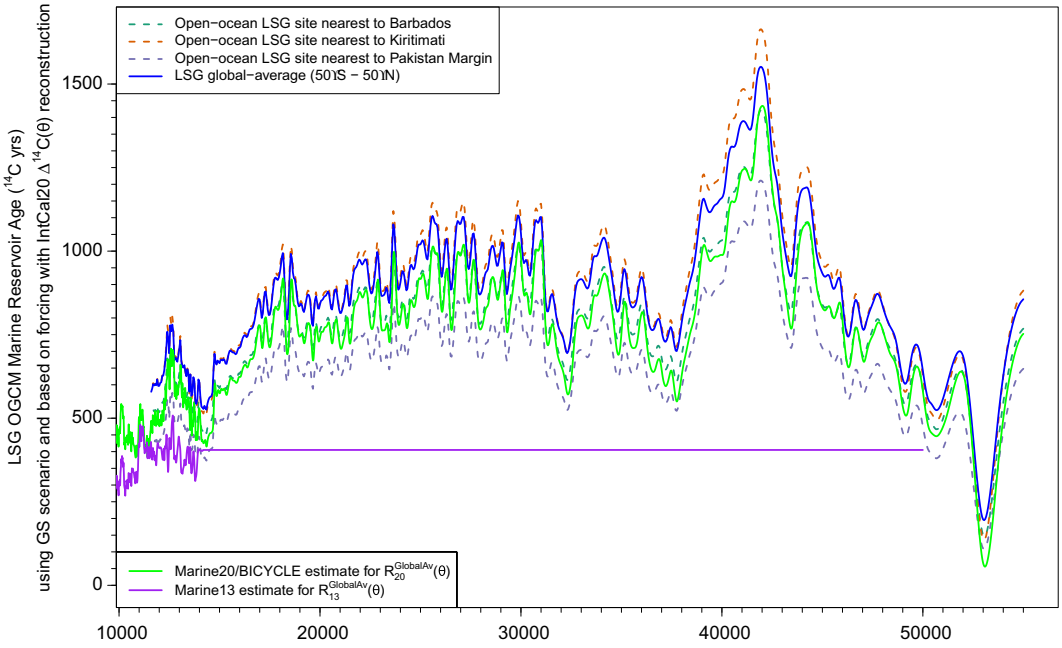

Figure 2 Plot of the mean Marine20 (BICYCLE-based) global-scale estimate of $R_{20}{}^{GlobalAv}(\theta)$, shown as green-solid line, against the LSG OGCM estimate of the overall MRA at three specific locations under its GS scenario and the LSG OGCM average under the GS scenario from 50°S–50°N. This GS scenario is intended to represent a glacial scenario (Sarnthein et al. 2003; Butzin et al. 2020) although is not transient in climate. Note that the plotted LSG OGCM estimates include their corresponding ΔR term. As we can shift the Marine20 estimate in each location according to a local ΔR_{20} estimate, it is the relative shapes of the curves (rather than the offsets) which are of primary relevance for inference. We also show the Marine13 estimate $R_{13}{}^{GlobalAv}(\theta)$ in purple for comparison. (Please see online version for color figures.)

carbon cycle model BICYCLE (Köhler and Fischer 2004, 2006; Köhler et al. 2005, 2006) to estimate the ocean's ^{14}C levels. BICYCLE is able to incorporate important time-dependent changes in the global carbon cycle. This was not possible with the box model used for Marine13 (Oeschger et al. 1975). The improvements in Marine20 are mainly seen in the period from 55,000–10,500 cal yr BP, in particular from 55,000–14,190 cal yr BP. There are however also some differences in the implementation of the Marine20 model compared to the Marine13 box model for the period 10,500–0 cal yr BP. See Figure 1a and Figure 2.

We know that from 55,000–10,500 cal yr BP there have been significant changes in global CO_2 concentration, related to substantial changes to the carbon cycle, as well as differences in global-average wind speeds compared with the recent past (Petit et al. 1990; McGee et al. 2010; Böhm et al. 2015; Köhler et al. 2017). We also know that these factors must have affected the MRA. However, it was not possible to include these changes in the computational modeling of Marine13 (Reimer et al. 2013). From 14,190–10,500 cal yr BP, Marine13 used a small set of marine records from tropical and subtropical locations to try and incorporate these changes from observational records. However, the Marine13 curve made no attempt to model *global-scale* changes in MRA from 55,000–14,190 cal yr BP. Marine13 set $R_{13}{}^{GlobalAv}(\theta)$ to be constant 405 ^{14}C yrs throughout this period (Figures 1a and 2).

https://doi.org/10.1017/RDC.2022.66 Published online by Cambridge University Press

When using Marine13, any MRA changes from 55,000–14,190 cal yr BP had to be entirely incorporated in the local $\Delta R_{13}(\theta)$, conflating *global-scale* and *localized* effects. If you were calibrating a ^{14}C sample and did not know how $\Delta R_{13}(\theta)$ changed over time, then you still had to model it as constant. This meant, with Marine13, you were effectively assuming there had been no variation in oceanic ^{14}C depletion from 55,000–14,190 cal yr BP. This is clearly incorrect, not least as the substantial changes in atmospheric ^{14}C levels (Reimer et al. 2020) would have affected the MRA.

Marine20 offers an improvement from 55,000–10,500 cal yr BP by incorporating, through usage of the BICYCLE model (Köhler and Fischer 2004, 2006; Köhler et al. 2005, 2006), as many of the known, and shared, *global-scale* palaeoclimate and carbon cycle changes that might influence oceanic ^{14}C depletion as currently possible. These large-scale carbon cycle changes are included in our estimate of ${R_{20}}^{GlobalAv}(\theta)$, and hence also the Marine20 curve (Figures 1 and 2). This enables better separation of *global* and *local* effects. Marine20 aims to model the effect of the changing global CO_2 concentration, atmospheric ^{14}C, wind speed, and basic carbon cycle changes in ocean circulation. Consequently, when using Marine20 we hope to have better accounted for the known effects of the global carbon cycle, and the damping of the atmospheric ^{14}C variations inherent to the ocean environment.

For the 10,500–0 cal yr BP period, Marine20 also aims to provide some small improvements in its estimate of ${R_{20}}^{GlobalAv}(\theta)$, and hence in the calibration curve, compared to the previous ${R_{13}}^{GlobalAv}(\theta)$ and Marine13 (see Figure 1). These are primarily due to an increased understanding of atmospheric ^{14}C production (since for Marine20 the model is forced by the improved IntCal20 curve rather than IntCal13) and the incorporation of more minor changes in global CO_2 concentration. Note that, when comparing Marine20 [and ${R_{20}}^{GlobalAv}(\theta)$] against Marine13 [and ${R_{13}}^{GlobalAv}(\theta)$] it is their relative changes over time which are important, not their absolute values. The curves aim to represent *global-scale* temporal effects, rather than a specific spatial average. The ~150 ^{14}C yrs offset between the Marine20 and Marine13 versions in the recent past is not therefore of direct relevance for comparisons. This offset will be accounted for in the changes from ΔR_{13} to ΔR_{20}. We discuss this further in Section 3.1.3.

2.3 Why Does This Marine20 Improvement Matter for a ^{14}C User?

For those seeking to obtain spatial understanding of MRAs to study the carbon cycle, the use of Marine20 makes it easier to compare MRA estimates in different locations—in particular, when the reference ^{14}C data are not all of the same calendar age. For those aiming to understand more detailed temporal MRA changes, comparison against Marine20 allows one to factor out the oceanic smoothing of rapid changes in atmospheric ^{14}C production rate and remove the effects of the global carbon cycle—any further MRA changes can therefore be identified as due to other time-varying factors. Conversely, a user studying spatial and temporal variations in the offset between the Marine13 curve and ^{14}C samples during the period from 55,000–14,190 cal yr BP could not disentangle local ocean reservoir changes from globally-shared effects. This hindered useful inference when comparing marine ^{14}C samples from the glacial period against Marine13 and earlier marine calibration curves. With these previous marine calibration curves, users had to estimate themselves whether the changes they saw in $R^{Location}(\theta)$ in the last glacial were due to global changes in atmospheric CO_2 partial pressure or in wind strength; or whether they were caused by

https://doi.org/10.1017/RDC.2022.66 Published online by Cambridge University Press

changes in ocean ventilation (e.g., Bard et al. 1994; Sikes et al. 2000; Siani et al. 2001). This is now addressed by estimating the offset $\Delta R_{20}(\theta)$ against Marine20.

For users calibrating new marine ^{14}C samples from a given location, the benefit of Marine20 can be seen by considering the two potential sources of errors when using any marine calibration curve from the IntCal project:

a. Error when modeling the *global-scale* MRA effects $R^{GlobalAv}(\theta)$;
b. Error in modeling the local MRA effects $\Delta R(\theta)$ as constant—in any region there are likely to be local factors affecting the MRA which aren't seen on a global level and which change over time, e.g., appearance and disappearance of sea-ice, and short-term local changes in circulation and upwelling.

Since Marine13 modeled ${R_{13}}^{GlobalAv}(\theta)$ as constant from 55,000–14,190 cal yr BP, the use of Marine13 for calibration of samples from this period will introduce significant errors of type (a). Conversely, the use of Marine20, with a variable ${R_{20}}^{GlobalAv}(\theta)$ that incorporates the effect of known *global-scale* variables on ^{14}C depletion, will reduce the magnitude of this type of error and so should improve calibration reliability. In the period from 14,190–0 cal yr BP, the differences between using Marine13 and Marine20 will typically be much smaller—so long as one ensures they update the estimate of ΔR_{13} to ΔR_{20}. We note that for both Marine13 and Marine20, potential error of type (b) will remain where there is temporal variation in regional factors that affect the local ^{14}C depletion but not the wider ocean. Without better understanding of regional effects, for which more detailed regional archives will likely be needed as discussed in Section 2.1.3, this type (b) error will remain somewhat irreducible.

3 QUESTIONS ON THE CONSTRUCTION OF MARINE20

3.1 Comparisons of Marine20 with Marine13

3.1.1 Have we changed our approach for Marine20, and if so, why?

The fundamental idea of the marine calibration curve has not changed between Marine20 and the earlier Marine curves. Both Marine20 and Marine13 use, where possible, an ocean-atmosphere computer model to estimate the changes in the MRA at the surface ocean which occur at a *global-scale*, i.e., $R^{GlobalAv}(\theta)$, and simultaneously use this estimate to generate a *global-scale* oceanic calibration curve which factors out $R^{GlobalAv}(\theta)$.

However, for Marine13, and the preceding marine calibration curves, these ocean-atmosphere computer models could not be extended back beyond 10,500 cal yr BP since they were not able to incorporate the carbon cycle and climate changes which are known to have occurred before then (Petit et al. 1990; McGee et al. 2010; Böhm et al. 2015; Henry et al. 2016; Köhler et al. 2017; Bauska et al. 2021). Significant simplifications were therefore required from 55,000–10,500 cal yr BP. With Marine20, through use of the carbon cycle box model BICYCLE (Köhler et al. 2006), we have been able to extend the computational modeling approach back to 55,000 cal yr BP and include more detailed knowledge regarding observed changes in the global carbon cycle. Hopefully, Marine20 therefore incorporates an improved estimate of the *global-scale* MRA effects which also extends back further in time.

3.1.2 What was done for Marine09 and Marine13?

For both Marine09 (Reimer et al. 2009) and Marine13 (Reimer et al. 2013), the curve from 10,500–0 cal yr BP was based upon a simple ocean-atmosphere box-diffusion model

https://doi.org/10.1017/RDC.2022.66 Published online by Cambridge University Press

(Oeschger et al. 1975). This box-model approach had been taken since 1986 (Stuiver et al. 1986). The available tree-ring ^{14}C data were used as the atmospheric model input, and parameters for air-sea gas exchange and eddy diffusivity were set to hit pre-bomb ^{14}C targets for the surface and deep ocean. This resulted in an estimate of the *global-scale* MRA ${R_{13}}^{GlobalAv}(\theta)$ (see Figure 1a) that was variable from 10,500–0 cal yr BP. However, in this time period, the variation is relatively small since the climate state was relatively constant, and carbon cycle (atmospheric CO_2) changes were minor.

For the portion of the Marine13 curve from 14,190–10,500 cal yr BP, Marine13 was based on a small set of, tropical and subtropical, coral and sediment records. This limited marine data was combined using the same statistical methodology as for IntCal13 (Niu et al. 2013) with the mean MRA for each site calculated from the overlap with the tree-rings. From 50,000–14,190 cal yr BP there were no tree-rings for calculating a *global-scale* MRA so a constant value of 405 ^{14}C yrs was applied (Figure 2) even though it was recognized that the use of a constant value wasn't correct because large *global-scale* MRA changes must have occurred.

The constant value of 405 ^{14}C yrs used for ${R_{13}}^{GlobalAv}(\theta)$ from 50,000–14,190 cal yr BP has remained the same since Marine04 (Hughen et al. 2004b) and was chosen to match the output of the Marine04 box-diffusion model output between AD 1350–1850. This model value is essentially the same as those used for calibrations before IntCal04 by Stuiver et al. (1986) (409 yr), by Stuiver and Braziunas (1993) (402 yr), and Stuiver et al. (1998) (400 yr). Since the carbon cycle was considerably different pre-Holocene compared with AD 1350–1850, such an estimate of $\approx$ 400 ^{14}C yrs is likely to be highly inappropriate between 50,000–14,190 cal yr BP during the last glaciation.

3.1.3 But has the Marine20 curve not meant that calibration and overall MRA estimates have changed significantly from Marine13 even in the Holocene?

In the Holocene, the *global-scale* Marine20 curve [and accompanying ${R_{20}}^{GlobalAv}(\theta)$] is offset by ~150 ^{14}C yrs from the Marine13 curve [and corresponding ${R_{13}}^{GlobalAv}(\theta)$]—see Figure 1b. However, this does not mean the estimate for the overall ^{14}C depletion in any specific oceanic location has changed substantially in the time period up until 10,500 cal yr BP.

The $R^{GlobalAv}(\theta)$ is poorly named. Rather than denoting the *global-average* MRA, it is more helpful to consider it as an estimate of ***global-scale* MRA changes**. It is the shape of this estimate, and specifically how it varies over time, which is important. As described in Section 1.1, the overall ^{14}C depletion in any oceanic location is a combination of the *global-scale* factors and the local variation. The total depletion at a marine site is

$$R^{Location}(\theta) = R^{GlobalAv}(\theta) + \Delta R^{Location}.$$

Consequently, if we introduce a constant shift to an estimate of $R^{GlobalAv}(\theta)$ this can be compensated for by simply reducing each $\Delta R^{Location}$ by the same amount (in the case of Marine20 and Marine13 this shift is ~150 ^{14}C yrs at 0 cal yr BP).

Marine13 and Marine20 [and their *global-scale* estimates, ${R_{13}}^{GlobalAv}(\theta)$ and ${R_{20}}^{GlobalAv}(\theta)$] are offset since they rely on different carbon cycle models. However, critically they have the same fundamental shape back to 10,500 cal yr BP (Figures 1a and b, also Figure 7 in Heaton et al. 2020). Once one factors in the updated ΔR_{20} values for the Marine20 curve, the effect on calibration and the overall MRA estimate in any specific location between the 2013 and

https://doi.org/10.1017/RDC.2022.66 Published online by Cambridge University Press

2020 marine calibration curves is generally relatively small back to 10,500 cal yr BP. It is however essential to update the estimates of ΔR, from ΔR_{13} to ΔR_{20}, for any location whenever one uses Marine20.

3.1.4 Why do we have to update our ΔR values, from ΔR_{13} to ΔR_{20}? Could we not have kept the same global-scale MRA changes?

The aim of the Marine calibration curve is to factor out *global-scale* carbon cycle changes as best one can. Marine20, through use of BICYCLE (Köhler et al. 2006), incorporates a more accurate estimate of these *global-scale* MRA changes than the previous marine calibration curves. Even in the Holocene, although differences to Marine13 are smaller (Figure 1b), the improved carbon cycle knowledge included in Marine20 should still increase our ability to resolve changes in MRA and improve marine calibrations.

As explained above, any constant shift in $R^{GlobalAv}(\theta)$ can be compensated for by applying the opposite shift to ΔR. It would therefore have been possible to shift Marine20 by a constant so that it agreed with the Marine13 curve at 0 cal yr BP; or so that ${R_{20}}^{GlobalAv}(\theta)$ agreed with the 405 ^{14}C yr box-model mean of previous Marine curves between AD 1350–1850. However, the unshifted Marine20, with a mean ${R_{20}}^{GlobalAv}(\theta)$ of 585 ^{14}C yrs between AD 1350–1850, was seen to fit marine ^{14}C samples from the recent past better than the Marine13 curve—see Figs. 9A and 9B in Heaton et al. (2020). We therefore left Marine20 and ${R_{20}}^{GlobalAv}(\theta)$ unshifted. Some hesitation remained about this choice, but it was felt preferable over an ad-hoc correction which would have maintained mostly positive ΔRs throughout the modern ocean (not only at high latitudes).

Furthermore, we note that estimates of ΔR values are frequently based on ^{14}C data from calendar years other than 0 cal yr BP (see later Figure 3). Even with an ad-hoc shift to match the Marine20 and Marine13 curves at 0 cal yr BP, the curves would not generally align at any other point in time. Recalculation of ΔR would still therefore be required in most cases. Additionally, since the uncertainty on the Marine20 curve is not identical to Marine13, updating of the ΔR estimates (to ΔR_{20}) would still be needed.

3.1.5 Are there situations where I should still use Marine13?

No, we do not recommend the continued use of Marine13. While we warned that Marine20 is not suitable for calibration in polar regions (Heaton et al. 2020), this is not resolved (and is in fact made worse) by using an earlier marine calibration curve such as Marine13. Similar warnings were provided in the earlier calibration papers although less explicitly (e.g., Reimer et al. 2013).

As described in Section 2.1.2, the issue in the polar regions is that during glacial periods, currently unknown local effects (e.g., changes in local sea-ice cover, strong winds, and altered ocean circulation) might have caused considerable localized, and short-term, changes in the surface ocean ^{14}C depletion (Butzin et al. 2017). These localized effects may have been distinct from those occurring on a global scale. Consequently, the assumption of an approximately constant $\Delta R(\theta)$ cannot be justified in polar regions before the onset of the Holocene. This problem of additional localized, and short-term, variations in ^{14}C depletion is not addressed by Marine13 or any of the earlier Marine calibration curves provided by the IntCal working group, and their use will not offer any improvements.

https://doi.org/10.1017/RDC.2022.66 Published online by Cambridge University Press

3.1.6 What should I do when calibrating marine ^{14}C samples from polar regions?

Until our knowledge of past climate and models improve, and we can provide regional calibration curves, the calibration of marine ^{14}C samples from polar regions, in particular during glacial periods, will remain a challenge.

Our cautious recommendation is that, if the sample is from the Holocene, one calibrate polar samples against Marine20 using a value of ΔR_{20} which is also based upon ^{14}C data from the Holocene. Ideally, one might estimate this ΔR_{20} based on samples of similar calendar age to that which one is calibrating. This recommendation is made on the assumption that, during the Holocene, variations in sea-ice cover and high-latitude winds that might affect ΔR_{20} should have remained small.

For polar ^{14}C samples dating from before the Holocene, when $\Delta R(\theta)$ may have varied significantly over time, great care must be taken in any calibration to prevent overconfidence in the calibrated date. Estimates of regional marine ^{14}C depletion are available under fixed carbon cycle and climate scenarios using the three-dimensional LSG ocean general circulation model (Butzin et al. 2020) on PANGAEA (https://doi.pangaea.de/10.1594/PANGAEA.914500), however these scenarios are not transient in terms of climate. Hence calibrating against any individual scenario is still likely to lead to overconfidence.

The Marine20 group have proposed that a user calibrate polar samples against latitudinal-specific *maximum-depletion* and *minimum-depletion* curves separately and use two resultant ages to inform a bracketing which it is hoped encompasses the true calendar age (Heaton et al. 2022). These bracketing calendar age intervals are however wide—with differences of up to 1500 calendar years between the *maximum-* and *minimum-depletion* calibration scenarios. As more information becomes available on polar palaeoclimate and the extent of sea-ice, we expect calibration in these regions will become more precise.

3.2 Construction of the Marine20 Curve

3.2.1 Why did you choose the BICYCLE model to make Marine20 rather than other models?

The BICYCLE model (Köhler et al. 2006) was chosen since it has sufficient complexity to accurately model the effect of a transient *global-scale* carbon cycle, yet remains sufficiently fast to be run hundreds of times and allow the uncertainty in the precise changes to the carbon cycle to be propagated though to Marine20.

For radiocarbon calibration, it is important not just to have a single *best* estimate for the calibration curve but to also understand the uncertainty around that curve. In the case of a model-based Marine calibration curve, uncertainty arises from two sources (Kennedy and O'Hagan 2001). Firstly, no computer model can perfectly represent the complexities of the Earth system. All models are simplifications and hence have a *model discrepancy uncertainty*. Secondly, the palaeoclimatic and carbon cycle changes we wish to feed into our ocean-atmosphere computer model are themselves somewhat uncertain. This uncertainty must be propagated through the model and introduces an *input-related uncertainty* to the Marine calibration curve.

Since carbon cycle models are complex and non-linear, we cannot reliably understand the *input-related uncertainty* by just running the model at the extremes of its climate and carbon cycle scenarios. Instead, we need to sample a range of scenarios from those that are

https://doi.org/10.1017/RDC.2022.66 Published online by Cambridge University Press

potentially feasible and run each through the computer model. This creates an ensemble of possible Marine curves. We can then infer the *input-related uncertainty* using Monte-Carlo from the variability between the individual Marine curves in the ensemble. In the case of Marine20, we created 500 possible, BICYCLE-based, Marine curves for our ensemble by varying BICYCLE's inputs according to our prior beliefs regarding their potential values.

While BICYCLE is a box-model, rather than a more complex Ocean General Circulation Model (OGCM), we believe it is sufficiently detailed to enable accurate modeling of large-scale MRA changes. We see little difference between the relative shapes of the BICYCLE-generated $R_{20}^{GlobalAv}(\theta)$ and the regional MRA estimates provided by the LSG OGCM (Butzin et al. 2020) as shown in Figure 2—see also Figure 4 in Heaton et al. (2020). This suggests that BICYCLE is able to capture most of the *global-scale* MRA temporal variations, and hopefully indicates that its *model discrepancy uncertainty* is small.

BICYCLE is also ideally suited to allow the Monte-Carlo approach required to understand the *input-related uncertainty* since it runs quickly. A more complex OGCM model, that could only be run very few times, would be of limited use for our Marine20 purposes. The use of BICYCLE allows Marine20 to provide good model representation yet still capture the significant *input-related uncertainty* which results from our lack of precise knowledge on the true palaeoclimate and carbon cycle inputs.

3.2.2 How did you choose the BICYCLE parameters?

The parameters in the BICYCLE model were not specifically tuned for Marine20. We took the same BICYCLE settings as had been used in a previous application of the model on ^{14}C dynamics (Köhler et al. 2006). A detailed description of the changing physical boundary conditions, based on palaeodata, that were prescribed for our implementation of BICYCLE can be found within Köhler et al. (2006)—specifically sea level, temperature, large scale ocean circulation, sea ice, and iron input which affects Southern Ocean marine biology. The parameters for BICYCLE were chosen to generate output that matched, as closely as possible, data-based reconstructions of changes in the carbon cycle during the past glacial cycle. This tuning focussed primarily on atmospheric CO_2 concentration, but also considered the fit to $\delta^{13}C$ and $\Delta^{14}C$ in the atmosphere. Further details can be found in Köhler et al. (2005).

For the creation of Marine20, the only three adjustments to the version of BICYCLE used in Köhler et al. (2006) were (i) a revised scheme for the implementation of carbonate compensation (i.e., the fluxes of carbonate ions between deep ocean and sediments); (ii) the external prescription of atmospheric CO_2 concentration, as opposed to using the values BICYCLE internally generates. This violates mass conservation but brings the carbon cycle as close as possible to the observational data; and (iii) the external prescription of atmospheric $\Delta^{14}C$—individual posterior realisations of the IntCal20 curve were used, avoiding any assumptions on ^{14}C production rates and enabling the propagation of uncertainty on atmospheric $\Delta^{14}C$ levels through to the Marine20 curve. More detail on these adjustments are provided in Heaton et al. (2020). During previous studies using BICYCLE, oceanic information on carbon cycle changes were also used to evaluate model performance, e.g., the deglacial changes in the vertical gradient of $\delta^{13}C$ in the Southern Ocean (Hodell et al. 2003).

https://doi.org/10.1017/RDC.2022.66 Published online by Cambridge University Press

The CO_2 concentration record used to force the BICYCLE model for Marine20 was a spline through data from six Antarctic ice cores on their most recent age models (Law Dome, WAIS Divide, EPICA Dome C, EPICA Dronning Maud Land, Siple Dome, Talos Dome). All details on data selection and the spline calculation are contained in Köhler et al. (2017).

4 QUESTIONS ON THE USE OF THE MARINE20 CURVE

4.1 Recalculating ΔR with the Marine20 curve

Whenever a new marine calibration curve is produced, a user will need to update the estimates of the additional regional components of MRA variation, i.e., the location specific $\Delta R(\theta)$, before using the curve. We describe below how to do this using contemporary samples in the marine radiocarbon reservoir database hosted at http://calib.org/marine/ and with a user's own ^{14}C reference data. Typically, the samples in the reservoir database have calendar ages varying from ca. 200–0 cal yr BP. If a user has their own ^{14}C samples from which to estimate ΔR, they can be of any calendar age.

As emphasized in Section 1.2.2, those users wishing to calibrate new ^{14}C samples should ideally obtain estimates of ΔR in their location from samples of a similar calendar age to those they intend to calibrate—for example using paired terrestrial and oceanic samples, or samples for which an independent calendar date is available. However, we recognize this is often not possible and ^{14}C data from the recent past is all that is available to estimate ΔR. In such cases, users should however give careful consideration as to whether, for the specific ocean location under study, an estimate of ΔR based on samples from the recent Holocene is suitable for calibration in much older time periods, and in particular the last glacial. This is especially relevant if the samples lie at higher latitudes, or within seas where ocean depth may have varied considerably. See Sections 2.1 and 4.2 for further discussion of these issues.

Users should also be aware that new samples are frequently added to the http://calib.org/marine/ radiocarbon reservoir database. As such new ^{14}C data become available, estimates of ΔR_{20} provided by the database may change. When calibrating, it is therefore important to note both the date of ΔR_{20} calculation and the references used.

If no information is available on how a previous ΔR_{13} was calculated, other than it was based on modern-day samples, we suggest a user can obtain an approximate ΔR_{20} by subtracting 150 ^{14}C yrs (the approximate offset between the mean of Marine13 and Marine20 in the period from 200–0 cal yr BP) from the published value of ΔR_{13}, i.e., setting $\Delta R_{20} = \Delta R_{13} - 150$ ^{14}C yrs. To prevent the need for this approximation going forward, we recommend all authors provide sufficient detail on how their estimates of ΔR were created to ensure reproducibility for future calibration curve updates.

4.1.1 Recalculating a constant ΔR_{20} based on data from the marine radiocarbon reservoir database

When we do not have detailed information on the changes in $\Delta R(\theta)$ over time, if we want to calibrate new ^{14}C samples we are required to make an approximation that it is constant, or at most slowly varying, for a given region. We can estimate this constant value ΔR_{20} from the difference in ^{14}C yrs of known age marine samples from that region and the Marine20 curve for that calendar age.

https://doi.org/10.1017/RDC.2022.66 Published online by Cambridge University Press

The ΔR values in the marine radiocarbon reservoir database at http://calib.org/marine/ (Reimer and Reimer 2001) have been recalculated to provide a ΔR_{20} for use with Marine20. We consider, as an example, estimating ΔR_{20} in the ocean region off the coast of Dublin (53.35°N, 6.26°W). The locations of the 10 nearest marine ^{14}C samples are shown in Figure 3. Some care should be taken when selecting which of the samples to use in estimating ΔR_{20} for a given location. Samples from restricted sites, such as lagoons or fjords, may not be appropriate for more open ocean locations. Suspension feeding organisms usually provide a more accurate representation of the surface ocean age than deposit feeders. Migratory species may not have fed at the site where they were collected. The weighted mean and uncertainty of selected samples can be calculated for use in calibration. Note that the number of locations can be specified and additional information, such as collection year (given in AD/BC) and feeding type, can be requested from the menu at the left.

In Figure 4, we plot the Marine20 curve and the ten ^{14}C observations identified in the map of Figure 3 which have been selected from the marine radiocarbon reservoir database. We calculate the offset between the curve and the samples in the calendar year of each ^{14}C sample. These provide estimates of $\Delta R_{20}(\theta)$ and may be used to give some indication of how reliable an assumption that it remains approximately constant over time is.

In the case we wish to approximate $\Delta R_{20}(\theta)$ as constant, e.g., to allow calibration of unknown age samples, then these values can be suitably averaged. In this case we get an estimate for ΔR_{20} of -201 ± 46 ^{14}C yrs (1σ). These calculations are all performed online within the marine radiocarbon reservoir database.

4.1.2 Recalculating a constant ΔR_{20} based on own reference ^{14}C samples

If a user has their own ^{14}C dated samples they can calculate a ΔR_{20} using the link to the *deltar* software (Reimer and Reimer 2017). These samples can be of known collection ages; independently dated ages, such as via U-Th or optically stimulated luminescence (OSL) dating; or contemporaneous marine and terrestrial radiocarbon ages including radiocarbon dated tephra deposits. The software will provide the 68% (1σ) and 95% (2σ) confidence intervals for ΔR_{20}. Most calibration programs expect a 68% (1σ) uncertainty on ΔR.

4.2 What Should a User Do if They Think ΔR has Changed Significantly from the Present-Day Values?

The assumption that modern-day ^{14}C samples are representative of $\Delta R(\theta)$ at times a long way further back in the past, i.e., a constant ΔR, should rightly be treated with caution. It is only proposed in situations where no more detailed information on changes in $\Delta R(\theta)$ is available. If such data is available, we recommend calculation of a ΔR_{20} using ^{14}C samples of a similar calendar age to those that one wishes to calibrate. Using such contemporaneous samples should provide an improved estimate of ΔR_{20} for the time period of the sample you wish to calibrate.

If a user is calibrating a ^{14}C sample for which they believe that there may be additional variation in $\Delta R(\theta)$, but does not have contemporaneous reference data on which to estimate the relevant value, they may wish to add an additional uncertainty to the present-day ΔR_{20} estimate before calibration.

https://doi.org/10.1017/RDC.2022.66 Published online by Cambridge University Press

Connected to marine20 database

Reset

Zoom and Pan to desired location, CLICK, Get Data, and hover your mouse over markers

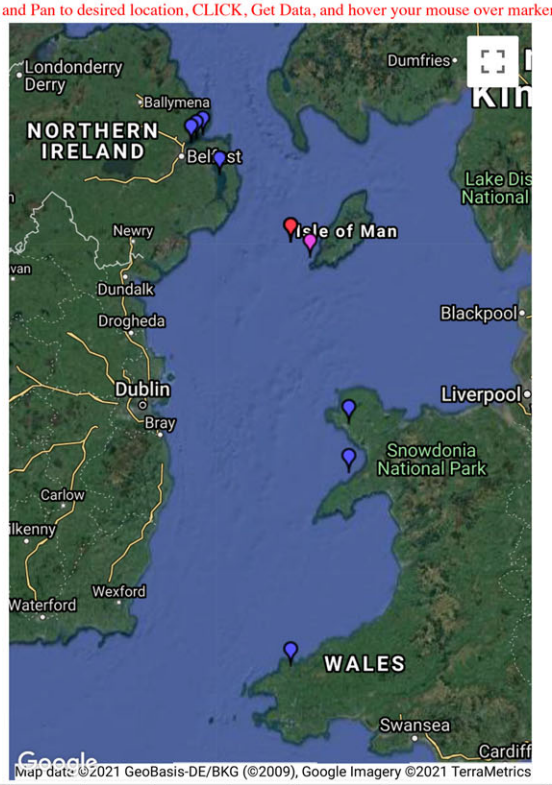

Get Data from

10 Nearest points

53.3498 centered @ lat

-6.2603 centered @ lon

- Subregion
- Notes
- CollectionYear
- ReservoirAge
- ReservoirErr
- C14age
- C14err
- LabID
- Delta13C
- nextime
- last_changed
- Genus
- Species
- Feeding
- Name

	MapNo	Lon	Lat	DeltaR	DeltaRErr	Reference	Locality	distance (km)
☐	995	-5.6000	54.5000	-239	25	Blake, CB. 2:2005	Strangford Lough	135
☐	994	-5.8500	54.6600	-130	38	Blake, CB. 2:2005	Belfast Lough	148
☐	993	-5.8000	54.6800	-205	35	Blake, CB. 2:2005	Belfast Lough	151
☐	992	-5.7500	54.7000	-238	35	Blake, CB. 2:2005	Belfast Lough	154
☐	527	-5.0000	54.1700	-180	47	Harkness, D :1983	Northeast Atlantic	123
☐	528	-5.0000	54.1700	-129	63	Harkness, D :1983	Northeast Atlantic	123
☐	1220	-4.8333	54.0917	-245	35	Butler, Paul:2009	Isle of Man	125
☐	544	-4.5000	53.2500	-147	49	Harkness, D :1983	Northeast Atlantic	117
☐	526	-4.5000	53.0000	-179	45	Harkness, D :1983	Northeast Atlantic	124
☐	525	-5.0000	52.0000	-141	54	Harkness, D :1983	Northeast Atlantic	172

Calculate Average of ticked boxes ☐ Select All

Figure 3 Location of ^{14}C samples near Dublin taken from marine radiocarbon reservoir database (http://calib.org/marine/). Credit: Map data ©2021 GeoBasis-DE/BKG, Google Imagery ©2021 Terrametrics. Blue and red pushpins denote suspension and deposit feeding organisms, respectively, and purple are time histories rather than single determinations. Hovering over the different colored pushpins at the top of the webpage provides further definitions.

https://doi.org/10.1017/RDC.2022.66 Published online by Cambridge University Press

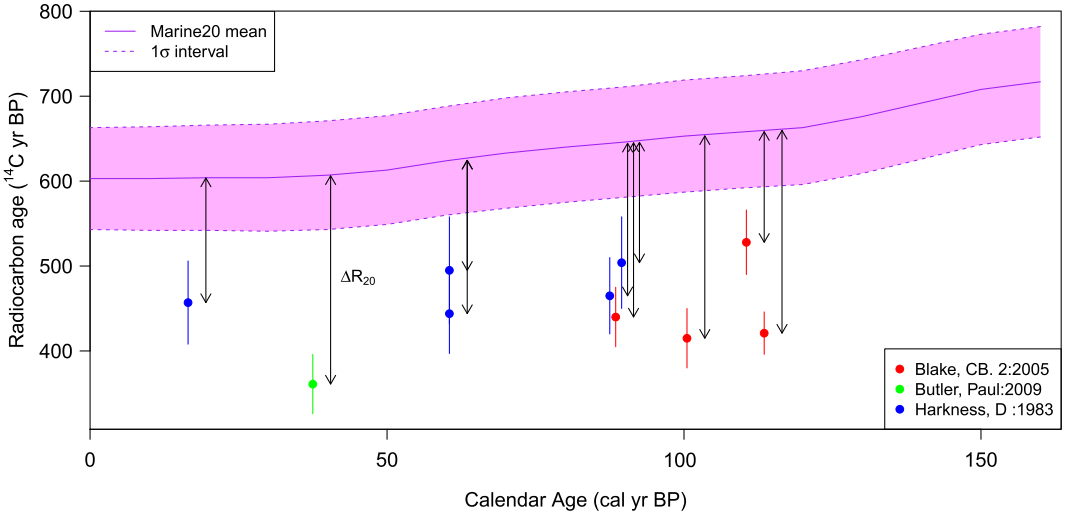

Figure 4 Known-age marine ^{14}C samples in the region off the coast of Dublin compared to the Marine20 calibration curve (shown in pink). We plot the 1σ-intervals on the ^{14}C observations and the Marine20 curve. The offsets, highlighted as arrows, form our estimate for $\Delta R_{20}(\theta)$ which we are typically required to assume as approximately constant to calibrate new, unknown age, marine ^{14}C samples from the region. (Please see online version for color figures.)

4.3 How should a user treat the MRA from the Southern Hemisphere?

Our definition of MRA, given in Section 1.1, considers the offset in radiocarbon years (^{14}C yrs) between the surface-layer dissolved inorganic carbon and the contemporaneous Northern Hemispheric atmosphere (Reimer et al. 2020). The Southern Hemispheric (SH) atmospheric ^{14}C level is somewhat offset, and depleted, compared to the Northern Hemispheric levels, with the SH atmosphere being 36 ± 27 ^{14}C yrs older (Hogg et al. 2020). This atmospheric offset changes over time and is known as the interhemispheric ^{14}C gradient.

If we are interested in assessing the level of ^{14}C disequilibrium between the surface-layer of site in the SH oceans and the SH atmosphere with which those sites directly interact, we must therefore be somewhat careful. By calculating the overall MRA at an ocean site with respect to the NH atmosphere, we will obtain MRAs at SH ocean sites that provide overestimates for the actual level of ^{14}C disequilibrium from the SH atmosphere. The size of this overestimate will be the value of the NH-SH atmospheric offset. Since Marine20 is created by forcing the BICYCLE model with the NH atmospheric, our estimates of $\Delta R_{20}(\theta)$ at SH ocean sites will also include a component caused by the NH-SH atmospheric offset rather than ocean changes.

When calibrating marine ^{14}C samples from the SH, one can still use the Marine20 curve so long as you estimate a $\Delta R_{20}(\theta)$ for the site. The effect of forcing Marine20 by the NH atmospheric ^{14}C levels, rather than the SH, should be compensated for through estimation of $\Delta R_{20}(\theta)$. This is not however the case if the MRA correction is based on, e.g., paired atmospheric-marine samples for the SH site.

https://doi.org/10.1017/RDC.2022.66 Published online by Cambridge University Press

We also note that there are hints that the interhemispheric ^{14}C gradient has varied in the past, notably due to winds and ocean changes (e.g., Rodgers et al. 2011; Capano et al. 2020). Hence, while those studying sites in the SH can still use the Marine20 curve since the interhemispheric offset is relatively small, more work is needed in the future to better constrain and reduce the uncertainties associated with the calibration of ^{14}C ages on marine samples.

5 ADDITIONAL QUESTIONS

5.1.1 Can I just calibrate my ^{14}C samples against the atmospheric IntCal20 curve directly using an estimate of the overall MRA $R^{Location}(\theta)$ for my region that I obtained from a particular calendar year (e.g., by looking at the offset to IntCal20 at 0 cal yr BP)?

No, using the atmospheric IntCal curves on ^{14}C samples from the open ocean directly isn't a reliable calibration approach and will result in incorrect calendar age estimate. One should always calibrate open ocean marine ^{14}C data against the Marine calibration curves using a regional ΔR adjustment rather than against an atmospheric calibration curve. The only exception to this is the case of ^{14}C samples from semi-closed basins, closed lakes and small seas, which we discuss in Section 5.1.3.

The marine (radiocarbon age vs. calendar age) ^{14}C calibration curve is not only offset from the atmospheric ^{14}C curve. As explained in Section 2, it is also much smoother as the ocean removes much of the high-frequency variation seen in the atmospheric ^{14}C signal and wiggles are somewhat delayed. Since the ocean responds more slowly to changes in ^{14}C production rates compared to the atmosphere, the overall MRA $R^{Location}(\theta)$ fluctuates very rapidly—such fluctuations in overall MRA occur when the atmospheric ^{14}C level has already changed but the ocean is still in the process of responding. This high-frequency variability in overall MRA can be clearly seen in the estimate of ${R_{20}}^{GlobalAv}(\theta)$, the *global-scale* temporal variations, plotted in Figure 1a. The necessary smoothing of the radiocarbon age vs. calendar age ^{14}C oscillations seen in the open ocean cannot be obtained with a constant overall MRA $R^{Location}(\theta)$. Such a constant $R^{Location}(\theta)$ would simply shift the atmospheric radiocarbon age vs. calendar age calibration curve but leave all the oscillations the same.

A user can estimate the total MRA, $R^{Location}(\theta)$, in a single calendar year by looking at the offset between IntCal20 and a specific ^{14}C sample. However, there is no guarantee that this single year estimate of total MRA will be representative of the total MRA for other calendar years due to this inherent smoothing of the atmospheric radiocarbon age vs. calendar age ^{14}C variations that occurs in the oceans. Such a user cannot therefore use their single-year point estimate of $R^{Location}(\theta)$ to calibrate new samples, of different calendar ages, against the atmospheric IntCal20 curve.

Marine20 models the damping present in the ocean during its construction, factoring out the high-frequency MRA changes in the resultant curve through its estimate of ${R_{20}}^{GlobalAv}(\theta)$. Figure 1a shows this ${R_{20}}^{GlobalAv}(\theta)$ during the Holocene. Most of the rapid variation shown here is a result of the smoothing, and delay, of the atmospheric IntCal20 ^{14}C signal that occurs in the ocean. Since, when using the Marine20 curve, the atmospheric damping has been factored out through the highly variable ${R_{20}}^{GlobalAv}(\theta)$, a user only needs to consider the additional local effects $\Delta R(\theta)$. These are less likely to relate to damping and so should hopefully remain more constant.

https://doi.org/10.1017/RDC.2022.66 Published online by Cambridge University Press

Further, there are physical reasons why changes in atmospheric CO_2, ^{14}C production and carbon cycle will significantly affect the MRA before the onset of the Holocene, typically increasing the level of oceanic ^{14}C depletion compared with the levels seen—again, see Figure 7 of Heaton et al. (2020). If one calibrates against Marine20 these effects are included. However, they are not if one simply applies a constant offset to the IntCal20 curve.

Finally, the use of MRA estimates based on previous iterations of Marine and IntCal curves will lead to incorrect inference. Each set of curve updates require the recalculation of MRA estimates.

5.1.2 How can a user get reference marine ^{14}C data from glacial periods to estimate a $\Delta R_{20}(\theta)$?

The Marine20 curve includes the *global-scale* changes in the MRA for glacial periods as discussed above. In most non-polar regions, we suggest this can be used together with an estimate of ΔR_{20} based upon independent marine ^{14}C from the recent past. Otherwise, it is very difficult unless you have paired marine/terrestrial ^{14}C dated material (see e.g., Petchey and Schmid 2020); a known-age tephra layer (Sikes et al. 2000; Siani et al. 2001); or a sample dated in some other way such as via U-Th or OSL (e.g., Toth et al. 2015, 2017; Hirabayashi et al. 2019; Hua et al. 2020). Note that while some of these references relate to data from the Holocene, the methods they desribe could also be applied to older samples. Stratigraphic alignment of cores to terrestrial records may also provide a method to estimate $\Delta R_{20}(\theta)$ and MRA (e.g., Muschitiello et al. 2019; Skinner et al. 2019; Waelbroeck et al. 2019; Brendryen et al. 2020).

5.1.3 How can I calibrate ^{14}C samples from closed seas and large lakes?

None of the Marine calibration curves are intended for closed seas and lakes. Closed seas and lakes have their own carbon turnover and reservoir offset that is independent of ocean circulation. Further complications arise, especially for lakes, since the ^{14}C offset between the surface water and the atmosphere is often affected by both the release of old (but not necessarily dead) organic carbon from soils and peats; and dead inorganic carbon (a hard water effect) entering the lake from its inflows/groundwater. The sensitivity to external inputs also depends on the lake's dissolved inorganic carbon which can vary widely, as well as the salinity from freshwater to hypersaline lakes. These are both fundamentally different from an open ocean reservoir age linked to ^{14}C decay during transport in a large water body and to limitations in the air-sea gas exchange.

Consequently, for the calibration of such samples, none of the Marine calibration curves are appropriate—they are based on open-ocean estimates of $R^{GlobalAv}(\theta)$ that include a large, ^{14}C-deficient, deep ocean reservoir. However, atmospheric IntCal calibration curves are also unlikely to be entirely appropriate for closed seas and large lakes since the carbon turnover will still smooth away at least some of the high-frequency (radiocarbon vs. calendar age) atmospheric variation. In reality, the damping with closed seas and large lakes is likely to lie somewhat between that seen in the (heavily damped) open-ocean Marine calibration curve and the (undamped) atmospheric calibration curve.

It is unfortunately not possible to give an off-the-shelf universal solution for those wishing to calibrate ^{14}C samples from non-open waters. We therefore defer to the user to decide upon, and justify, an appropriate approach to calibration based upon their expert knowledge of the

https://doi.org/10.1017/RDC.2022.66 Published online by Cambridge University Press

specific sea or lake. For large lakes and closed seas, hydrological modeling to determine the surface water ^{14}C depletion (using models without deep water compartments) may be most appropriate (e.g., Yu et al. 2007). For smaller lakes, where there are known age shells or other lacustrine organisms available, then the simplest approach would be to measure the ^{14}C ages of these samples and calculate the lake's offset to the atmospheric IntCal20 curve, with an estimated fossil fuel correction for post-industrial age samples. This atmospheric offset can then be used to calibrate other ^{14}C samples directly against the IntCal20 curve. This suggestion comes with considerable caveats however, since the ^{14}C reservoir offset in a lake can vary over time for many reasons including changing hydrological cycles. Paired terrestrial and lacustrine or sediment samples may therefore be needed throughout the core to determine the appropriate atmospheric ^{14}C offset to apply.

In the case of semi-closed basins (i.e., those which have sometimes been cut-off partially or completely from the open ocean, but at other times have not) a ^{14}C user must consider both the present open-ocean exchange and the time evolution of these exchanges due to past sea level changes. Complications will inevitably arise, ranging from basins that were completely disconnected during the LGM and Late Glacial (e.g., Baltic Sea, Black Sea) to basins in which hydrology was probably affected in a more subtle way (e.g., Mediterranean Sea, Red Sea, and Arctic Ocean with the closure of the Bering Strait). Again more research is needed to understand the evolution of reservoir ages in such semi-closed basins (e.g., of the Black Sea Soulet et al. 2011).

5.1.4 What should be done for ^{14}C samples that arise from different water masses such as the deep and intermediate ocean?

It is important to also stress that Marine20, and all previous marine calibration curves, are only useful for marine samples which grew at the ocean surface. As a community we are a great distance from being able to provide individual marine calibration curves for the deep and intermediate layers in the main ocean basins. Such work will require much more understanding of ocean circulation. Currently, deep sea corals and benthic foraminifera can provide data from different water masses.

5.1.5 How can a user propose ^{14}C data for inclusion in the marine reservoir database?

Researchers with either known age or independently dated pre-bomb ^{14}C measurements, which can be used to calculate ΔR_{20}, are encouraged to send published papers and relevant information to R. or P.J. Reimer for inclusion in the database. Please note however that, because of its setup, which assumes a known-age or independently dated sample with insignificant calendar age uncertainty, paired marine and terrestrial data cannot be included in the current radiocarbon reservoir database. The user can of course still calculate ΔR_{20} values for their own paired samples using the *deltar* software provided through the database.

5.1.6 What information should ^{14}C users include in their papers to ensure adherence to open science best practices?

Since all ^{14}C calibration curves are regularly updated, it is essential to ensure that calibration is reproducible, and critically that all calendar dates and inference can be revised, for future calibration curve updates. All ^{14}C users should therefore provide the conventional radiocarbon ages for their samples (in ^{14}C yr BP) and the accompanying lab codes. They

https://doi.org/10.1017/RDC.2022.66 Published online by Cambridge University Press

should also clarify which calibration curve they have used for the reader as advised by Millard (2014).

When linking and referencing research, users should also ensure that they are not comparing calendar dates, or inference, that have been obtained with different versions/updates of calibration curves. For example, it is not reliable to compare inference and calendar dates across papers which have been inconsistently calibrated, with some calendar age estimates being provided by calibration against IntCal/Marine09 while others have been estimated using IntCal/Marine13 and/or IntCal/Marine20.

In the case of the Marine calibration curves, this consistency is also important if estimating changes in $\Delta R_{20}(\theta)$ by looking at the offset against Marine20. One must not mix estimates of $\Delta R_{20}(\theta)$ with previous estimates of $\Delta R_{09}(\theta)$ or $\Delta R_{13}(\theta)$ that were obtained by looking at the offset to Marine09 or Marine13. This is particularly the case when studying changes in the last glacial period since Marine09 and Marine13 incorporated no global-scale carbon cycle changes (see Figure 2 and Section 3).

Authors are also encouraged to ensure that the method they used to estimate ΔR_{20} for calibration is entirely reproducible for future Marine calibration curve updates. This will require an explanation of the method used and referencing of the original publications in the marine database that have been used to determine ΔR_{20}.

5.1.7 Do all editors of all journals know that they have to check that the date of the marine database used has to be mentioned in the bibliographic reference, since it is continuously updated?

No, reviewers and editors will need to be encouraged to check that ΔR_{20} values have been used, either because the subscript is included or the date when the database was used is given.

ACKNOWLEDGMENTS

P. Köhler and M. Butzin are supported by the German Federal Ministry of Education and Research (BMBF), as Research for Sustainability initiative (FONA); www.fona.de through the PalMod project (grant numbers: 01LP1505B, 01LP1919A), which also covered the Open Access fees. E. Bard is funded by EQUIPEX ASTER-CEREGE and ANR MARCARA.

REFERENCES

Ascough PL, Cook GT, Dugmore AJ. 2009. North Atlantic marine ^{14}C reservoir effects: Implications for late-Holocene chronological studies. Quat. Geochronol. 4:171–180. doi: 10.1016/j.quageo.2008.12.002.

Bard E. 1988. Correction of accelerator mass spectrometry ^{14}C ages measured in planktonic foraminifera: paleoceanographic implications. Paleoceanography 3:635–645. doi: 10.1029/PA003i006p00635.

Bard E, Heaton TJ. 2021. On the tuning of plateaus in atmospheric and oceanic ^{14}C records to derive calendar chronologies of deep-sea cores and records of ^{14}C marine reservoir age changes. Clim. Past 17:1701–1725. doi: 10.5194/cp-17-1701-2021.

Bard E, Arnold M, Mangerud J, Paterne M, Labeyrie L, Duprat J, Mélières M-A, Sønstegaard E, Duplessy J-C. 1994. The North Atlantic atmosphere-sea surface ^{14}C gradient during the Younger Dryas climatic event. Earth Planet. Sci. Lett. 126:275–287. doi: 10.1016/0012-821X(94)90112-0.

Bauska TK, Marcott SA, Brook EJ. 2021. Abrupt changes in the global carbon cycle during the last glacial period. Nat. Geosci. 14:91–96. doi: 10.1038/s41561-020-00680-2.

van Beek P, Reyss J-L, Paterne M, Gersonde R, van der Loeff MR, Kuhn G. 2002. ^{226}Ra in barite: absolute dating of Holocene Southern Ocean sediments and reconstruction of sea-surface

https://doi.org/10.1017/RDC.2022.66 Published online by Cambridge University Press

reservoir ages. Geology 30:731–734. doi: 10.1130/0091-7613(2002)030<0731:RIBADO>2.0.CO;2.

Böhm E, Lippold J, Gutjahr M, Frank M, Blaser P, Antz B, Fohlmeister J, Frank N, Andersen MB, Deininger M. 2015. Strong and deep Atlantic meridional overturning circulation during the last glacial cycle. Nature 517:73–76. doi: 10.1038/nature14059.

Bondevik S, Mangerud J, Birks HH, Gulliksen S, Reimer P. 2006. Changes in North Atlantic radiocarbon reservoir ages during the Allerød and Younger Dryas. Science 312:1514–1517. doi: 10.1126/science.1123300.

Brendryen J, Haflidason H, Yokoyama Y, Haaga KA, Hannisdal B. 2020. Eurasian Ice Sheet collapse was a major source of Meltwater Pulse 1A 14,600 years ago. Nat. Geosci. 13: 363–368. doi: 10.1038/s41561-020-0567-4.

Burr GS, Vance Haynes C, Shen C-C, Taylor F, Chang Y-W, Beck JW, Nguyen V, Zhou W. 2015. Temporal variations of radiocarbon reservoir ages in the South Pacific Ocean during the Holocene. Radiocarbon 57:507–515. doi: 10.2458/azu_rc.57.18460.

Butzin M, Prange M, Lohmann G. 2005. Radiocarbon simulations for the glacial ocean: the effects of wind stress, Southern Ocean sea ice and Heinrich events. Earth Planet. Sci. Lett. 235:45–61. doi: 10.1016/j.epsl.2005.03.003.

Butzin M, Köhler P, Lohmann G. 2017. Marine radiocarbon reservoir age simulations for the past 50,000 years. Geophys. Res. Lett. 44:8473–8480. doi: 10.1002/2017GL074688.

Butzin M, Heaton TJ, Köhler P, Lohmann G. 2020. A short note on marine reservoir age simulations used in IntCal20. Radiocarbon 62:865–871. doi: 10.1017/RDC.2020.9.

Capano M, Miramont C, Shindo L, Guibal F, Marschal C, Kromer B, Tuna T, Bard E. 2020. Onset of the Younger Dryas recorded with ^{14}C at annual resolution in French subfossil trees. Radiocarbon 62:901–918. doi: 10.1017/RDC.2019.116.

Carré M, Jackson D, Maldonado A, Chase BM, Sachs JP. 2016. Variability of ^{14}C reservoir age and air–sea flux of CO2 in the Peru–Chile upwelling region during the past 12,000 years. Quat. Res. 85:87–93. doi: 10.1016/j.yqres.2015.12.002.

Druffel EM, Suess HE. 1983. On the radiocarbon record in banded corals: exchange parameters and net transport of $^{14}CO_2$ between atmosphere and surface ocean. J. Geophys. Res. Ocean 88:1271–1280. doi: 10.1029/JC088iC02p01271.

Grottoli AG, Eakin CM. 2007. A review of modern coral $\delta^{18}O$ and $\Delta^{14}C$ proxy records. Earth-Science Rev. 81:67–91. doi: 10.1016/j.earscirev.2006.10.001.

Heaton TJ, Köhler P, Butzin M, Bard E, Reimer RW, Austin WEN, Bronk-Ramsey C, Grootes PM, Hughen KA, Kromer B, Reimer PJ, Adkins J, Burke A, Cook MS, Olsen J, Skinner LC. 2020. Marine20—the marine radiocarbon age calibration curve (0–55,000 cal BP). Radiocarbon 62:779–820. doi: 10.1017/RDC.2020.68.

Heaton TJ, Butzin M, Bard E, Bronk Ramsey C, Hughen KA, Köhler P, Reimer PJ. 2022. Calibration in polar regions: an age bracketing approach for approximate calibration. EarthArXiv Preprint. doi: 10.31223/X5P92G

Henry LG, McManus JF, Curry WB, Roberts NL, Piotrowski AM, Keigwin LD. 2016. North Atlantic ocean circulation and abrupt climate change during the last glaciation. Science 353:470–474. doi: 10.1126/science.aaf5529.

Hirabayashi S, Yokoyama Y, Suzuki A, Esat T, Miyairi Y, Aze T, Siringan F, Maeda Y. 2019. Local marine reservoir age variability at Luzon Strait in the South China Sea during the Holocene. Nucl. Instruments Methods Phys. Res. Sect. B Beam Interact. with Mater. Atoms 455:171–177. doi: 10.1016/j.nimb.2018.12.001.

Hodell DA, Venz KA, Charles CD, Ninnemann US. 2003. Pleistocene vertical carbon isotope and carbonate gradients in the South Atlantic sector of the Southern Ocean, Geochemistry, Geophys. Geosystems 4:1–19. doi: 10.1029/2002GC000367.

Hogg AG, Heaton TJ, Hua Q, Palmer JG, Turney CSM, Southon J, Bayliss A, Blackwell PG, Boswijk G, Bronk Ramsey C, Pearson C, Petchey F, Reimer P, Reimer R, Wacker L. 2020. SHCal20 Southern Hemisphere calibration, 0–55,000 years cal BP. Radiocarbon 62:759–778. doi: 10.1017/RDC.2020.59.

Hua Q, Webb GE, Zhao J, Nothdurft LD, Lybolt M, Price GJ, Opdyke BN. 2015. Large variations in the Holocene marine radiocarbon reservoir effect reflect ocean circulation and climatic changes. Earth Planet. Sci. Lett. 422:33–44. doi: 10.1016/j.epsl.2015.03.049.

Hua Q, Ulm S, Yu K, Clark TR, Nothdurft LD, Leonard ND, Pandolfi JM, Jacobsen GE, Zhao J. 2020. Temporal variability in the Holocene marine radiocarbon reservoir effect for the Tropical and South Pacific. Quat. Sci. Rev. 249:106613. doi: 10.1016/j.quascirev.2020.106613.

Hughen KA, Lehman SJ, Southon JR, Overpeck JT, Marchal O, Herring C, Turnbull J. 2004a. ^{14}C activity and global carbon cycle changes over the past 50,000 years. Science 303:202–207. doi: 10.1126/science.1090300.

Hughen KA, Baillie MG, Bard E, Beck JW, Bertrand CJ, Blackwell PG, Buck CE, Burr GS, Cutler KB, Damon PE, Edwards RL, Fairbanks RG, Friedrich M, Guilderson TP, Kromer B, McCormac G, Manning S, Bronk Ramsey C, Reimer PA, Reimer RW, Remmele S, Southon JR, Stuiver M, Talamo S, Taylor FW, van der Plicht J, Weyhenmeyer CE. 2004b. Marine04

https://doi.org/10.1017/RDC.2022.66 Published online by Cambridge University Press

marine radiocarbon age calibration, 0–26 cal kyr BP. Radiocarbon 46:1059–1086. doi: 10.1017/S0033822200033002.

Kageyama M, Harrison SP, Kapsch M-L, Lofverstrom M, Lora JM, Mikolajewicz U, Sherriff-Tadano S, Vadsaria T, Abe-Ouchi A, Bouttes N, Chandan D, Gregoire LJ, Ivanovic RF, Izumi K, LeGrande AN, Lhardy F, Lohmann G, Morozova PA, Ohgaito R, Paul A, Peltier WR, Poulsen CJ, Quiquet A, Roche DM, Shi X, Tierney JE, Valdes PJ, Volodin E, Zhu J. 2021. The PMIP4 Last Glacial Maximum experiments: preliminary results and comparison with the PMIP3 simulations. Clim. Past 17: 1065–1089. doi: 10.5194/cp-17-1065-2021.

Kennedy MC, O'Hagan A. 2001. Bayesian calibration of computer models. J. R. Stat. Soc. Ser. B (Statistical Methodol.) 63:425–464. doi: 10.1111/1467-9868.00294.

Key RM. 2001. Radiocarbon. In: Encyclopedia of ocean sciences. Oxford: Academic Press. p. 2338–2353. doi: 10.1006/rwos.2001.0162.

Key RM, Kozyr A, Sabine CL, Lee K, Wanninkhof R, Bullister JL, Feely RA, Millero FJ, Mordy C, Peng T-H. 2004. A global ocean carbon climatology: results from Global Data Analysis Project (GLODAP). Global Biogeochem. Cycles 18: doi: 10.1029/2004GB002247.

Kohfeld KE, Graham RM, de Boer AM, Sime LC, Wolff EW, Le Quéré C, Bopp L. 2013. Southern Hemisphere westerly wind changes during the Last Glacial Maximum: paleo-data synthesis. Quat. Sci. Rev. 68:76–95. doi: 10.1016/j.quascirev.2013.01.017.

Köhler P, Fischer H. 2004. Simulating changes in the terrestrial biosphere during the last glacial/interglacial transition. Glob. Planet. Change 43:33–55. doi: 10.1016/j.gloplacha.2004.02.005.

Köhler P, Fischer H. 2006. Simulating low frequency changes in atmospheric CO_2 during the last 740 000 years. Clim. Past 2:57–78. doi: 10.5194/cp-2-57-2006.

Köhler P, Fischer H, Munhoven G, Zeebe RE. 2005. Quantitative interpretation of atmospheric carbon records over the last glacial termination. Global Biogeochem. Cycles 19. doi: 10.1029/2004GB002345.

Köhler P, Muscheler R, Fischer H. 2006. A model-based interpretation of low-frequency changes in the carbon cycle during the last 120,000 years and its implications for the reconstruction of atmospheric $\Delta^{14}C$. Geochemistry, Geophys. Geosystems 7. doi: 10.1029/2005GC001228.

Köhler P, Nehrbass-Ahles C, Schmitt J, Stocker TF, Fischer HA 2017. 156 kyr smoothed history of the atmospheric greenhouse gases CO_2, CH_2, and N_2O and their radiative forcing. Earth Syst. Sci. Data 9:363–387. doi: 10.5194/essd-9-363-2017.

Komugabe-Dixson AF, Fallon SJ, Eggins SM, Thresher RE. 2016. Radiocarbon evidence for mid-late Holocene changes in southwest Pacific Ocean circulation. Paleoceanography 31: 971–985. doi: 10.1002/2016PA002929.

Latorre C, De Pol-Holz R, Carter C, Santoro CM. 2017. Using archaeological shell middens as a proxy for past local coastal upwelling in northern Chile. Quat. Int. 427:128–136. doi: 10.1016/j.quaint.2015.11.079.

Levin I, Hesshaimer V. 2000. Radiocarbon—a unique tracer of global carbon cycle dynamics. Radiocarbon 42:69–80. doi: 10.1017/S0033822200053066.

Lindauer S, Santos GM, Steinhof A, Yousif E, Phillips C, Jasim SA, Uerpmann H-P, Hinderer M. 2017. The local marine reservoir effect at Kalba (UAE) between the Neolithic and Bronze Age: an indicator of sea level and climate changes. Quat. Geochronol. 42:105–116. doi: 10.1016/j.quageo.2017.09.003.

McGee D, Broecker WS, Winckler G. 2010. Gustiness: the driver of glacial dustiness? Quat. Sci. Rev. 29:2340–2350. doi: 10.1016/j.quascirev.2010.06.009.

McGregor HV, Gagan MK, McCulloch MT, Hodge E, Mortimer G. 2008. Mid-Holocene variability in the marine ^{14}C reservoir age for northern coastal Papua New Guinea. Quat. Geochronol. 3:213–225. doi: 10.1016/j.quageo.2007.11.002.

Millard AR. 2014. Conventions for reporting radiocarbon determinations. Radiocarbon 56: 555–559. doi: 10.2458/56.17455.

Muschitiello F, D'Andrea WJ, Schmittner A, Heaton TJ, Balascio NL, deRoberts N, Caffee M. W, Woodruff TE, Welten KC, Skinner LC, Simon MH, Dokken TM. 2019. Deep-water circulation changes lead North Atlantic climate during deglaciation. Nat. Commun. 10. doi: 10.1038/s41467-019-09237-3.

Niu M, Heaton TJ, Blackwell PG, Buck CE. 2013. The Bayesian approach to radiocarbon calibration curve estimation: the IntCal13, Marine13, and SHCal13 methodologies. Radiocarbon 55. doi: 10.2458/azu_js_rc.55.17222.

Oeschger H, Siegenthaler U, Schotterer U, Gugelmann A. 1975. A box diffusion model to study the carbon dioxide exchange in nature. Tellus 27:168–192. doi: 10.1111/j.2153-3490.1975.tb01671.x.

Oka A, Abe-Ouchi A, Sherriff-Tadano S, Yokoyama Y, Kawamura K, Hasumi H. 2021. Glacial mode shift of the Atlantic meridional overturning circulation by warming over the Southern Ocean. Commun. Earth Environ. 2:169. doi: 10.1038/s43247-021-00226-3.

Ortlieb L, Vargas G, Saliège J-F. 2011. Marine radiocarbon reservoir effect along the northern Chile–southern Peru coast (14–24°S) throughout the Holocene. Quat. Res. 75:91–103. doi: 10.1016/j.yqres.2010.07.018.

Petchey F. 2020. New evidence for a Mid- to Late-Holocene change in the marine reservoir effect

https://doi.org/10.1017/RDC.2022.66 Published online by Cambridge University Press

across the South Pacific Gyre. Radiocarbon 62:127–139. doi: 10.1017/RDC.2019.103.

Petchey F, Schmid MME. 2020. Vital evidence: change in the marine ^{14}C reservoir around New Zealand (Aotearoa) and implications for the timing of Polynesian settlement. Sci. Rep. 10:14266. doi: 10.1038/s41598-020-70227-3.

Petit JR, Mourner L, Jouzel J, Korotkevich YS, Kotlyakov VI, Lorius C. 1990. Palaeoclimatological and chronological implications of the Vostok core dust record, Nature 343:56–58. doi: 10.1038/343056a0.

Reimer PJ, Reimer RW. 2001. A Marine reservoir correction database and on-line interface. Radiocarbon 43:461–463. doi: 10.1017/S0033822200038339.

Reimer PJ, Baillie MGL, Bard E, Bayliss A, Beck JW, Blackwell PG, Bronk Ramsey C, Buck CE, Burr GS, Edwards RL, Friedrich M, Grootes PM, Guilderson TP, Hajdas I, Heaton T, Hogg AG, Hughen KA, Kaiser KF, Kromer B, McCormac FG, Manning SW, Reimer RW, Richards DA, Southon JR, Talamo S, Turney CSM, van der Plicht J, Weyhenmeyer CE. 2009. IntCal09 and Marine09 radiocarbon age calibration curves, 0–50,000 years cal BP. Radiocarbon 51(4):1111–1150. doi: 10.1017/s0033822200034202.

Reimer PJ, Bard E, Bayliss A, Beck JW, Blackwell PG, Bronk Ramsey C, Buck C, Cheng H, Edwards RL, Friedrich M, Grootes PM, Guilderson TP, Haflidason H, Hajdas I, Hatté C, Heaton TJ, Hoffmann DL, Hogg AG, Hughen KA, Kaiser KF, Kromer B, Manning SW, Niu M, Reimer RW, Richards DA, Scott EM, Southon JR, Staff RA, Turney CSM, van der Plicht J. 2013. IntCal13 and Marine13 radiocarbon age calibration curves 0–50,000 years cal BP. Radiocarbon 55(4):1869–1887. doi: 10.2458/azu_js_rc.55.16947.

Reimer PJ, Austin WEN, Bard E, Bayliss A, Blackwell PG, Ramsey CB, Butzin M, Cheng H, Edwards RL, Friedrich M, Grootes PM, Guilderson TP, Hajdas I, Heaton TJ, Hogg AG, Hughen KA, Kromer B, Manning SW, Muscheler R, Palmer JG, Pearson C, van der Plicht J, Reimer RW, Richards DA, Scott EM, Southon JR, Turney CSM, Wacker L, Adolphi F, Büntgen U, Capano M, Fahrni SM, Fogtmann-Schulz A, Friedrich R, Köhler P, Kudsk P, Miyake F, Olsen J, Reinig F, Sakamoto M, Sookdeo A, Talamo S. 2020. The IntCal20 Northern Hemisphere radiocarbon age calibration curve (0–55 cal kBP). Radiocarbon 62(4):725–757. doi: 10.1017/RDC.2020.41.

Reimer RW, Reimer PJ. 2017. An online application for ΔR calculation. Radiocarbon 59: 1623–1627. doi: 10.1017/RDC.2016.117.

Rodgers KB, Mikaloff-Fletcher SE, Bianchi D, Beaulieu C, Galbraith ED, Gnanadesikan A, Hogg AG, Iudicone D, Lintner BR, Naegler T, Reimer PJ, Sarmiento JL, Slater RD. 2011. Interhemispheric gradient of atmospheric radiocarbon reveals natural variability of Southern Ocean winds. Clim. Past 7:1123–1138. doi: 10.5194/cp-7-1123-2011.

Sarnthein M, Gersonde R, Niebler S, Pflaumann U, Spielhagen R, Thiede J, Wefer G, Weinelt M. 2003. Overview of Glacial Atlantic Ocean Mapping (GLAMAP 2000). Paleoceanography 18. doi: 10.1029/2002PA000769.

Siani G, Paterne M, Michel E, Sulpizio R, Sbrana A, Arnold M, Haddad G. 2001. Mediterranean Sea surface radiocarbon reservoir age changes since the Last Glacial Maximum. Science 294:1917–1920. doi: 10.1126/science.1063649.

Siani G, Michel E, De Pol-Holz R, DeVries T, Lamy F, Carel M, Isguder G, Dewilde F, Lourantou A. 2013. Carbon isotope records reveal precise timing of enhanced Southern Ocean upwelling during the last deglaciation. Nat. Commun. 4:2758. doi: 10.1038/ncomms3758.

Sikes EL, Samson CR, Guilderson TP, Howard WR. 2000. Old radiocarbon ages in the southwest Pacific Ocean during the last glacial period and deglaciation. Nature 405:555–559. doi: 10.1038/35014581.

Skinner L, Bard E. 2022. Radiocarbon as a dating tool and tracer in paleoceanography. Rev. Geophys. 60. doi: 10.1029/2020RG000720.

Skinner LC, Primeau F, Freeman E, de la Fuente M, Goodwin PA, Gottschalk J, Huang E, McCave IN, Noble TL, Scrivner AE. 2017. Radiocarbon constraints on the glacial ocean circulation and its impact on atmospheric CO_2. Nat. Commun. 8:16010. doi: 10.1038/ncomms16010.

Skinner LC, Muschitiello F, Scrivner AE. 2019. Marine reservoir age variability over the last deglaciation: implications for marine carboncycling and prospects for regional radiocarbon calibrations. Paleoceanogr. Paleoclimatology 34:1807–1815. doi: 10.1029/2019PA003667.

Soulet G, Ménot G, Garreta V, Rostek F, Zaragosi S, Lericolais G, Bard E. 2011. Black Sea "Lake" reservoir age evolution since the Last Glacial—hydrologic and climatic implications. Earth Planet. Sci. Lett. 308:245–258. doi: 10.1016/j.epsl.2011.06.002.

Stuiver M, Braziunas TF. 1993. Modeling atmospheric ^{14}C influences and ^{14}C ages of marine samples to 10,000 BC. Radiocarbon 35:137–189. doi: 10.1017/S0033822200013874.

Stuiver M, Pearson GW, Braziunas T. 1986. Radiocarbon age calibration of marine samples back to 9000 cal yr BP. Radiocarbon 28:980–1021. doi: 10.1017/S0033822200060264.

Stuiver M, Reimer PJ, Bard E, Beck JW, Burr GS, Hughen KA, Kromer B, McCormac G, van der Plicht J, Spurk M. 1998. INTCAL98 radiocarbon age calibration, 24,000–0 cal BP,

https://doi.org/10.1017/RDC.2022.66 Published online by Cambridge University Press

Radiocarbon 40:1041–1083. doi: 10.1017/S0033822200019123.

Telesiński MM, Ezat MM, Muschitiello F, Bauch HA, Spielhagen RF. 2021. Ventilation history of the Nordic Seas deduced from pelagic-benthic radiocarbon age offsets. Geochemistry, Geophys. Geosystems 22:e2020GC009132. doi: 10.1029/2020GC009132.

Toggweiler JR, Druffel ERM, Key RM, Galbraith ED. 2019. Upwelling in the ocean basins north of the ACC: 1. On the upwelling exposed by the surface distribution of $\Delta^{14}C$. J. Geophys. Res. Ocean. 124:2591–2608. doi: 10.1029/2018JC014794.

Toth LT, Aronson RB, Cheng H, Edwards RL. 2015. Holocene variability in the intensity of wind-gap upwelling in the tropical eastern Pacific. Paleoceanography 30:1113–1131. doi: 10.1002/2015PA002794.

Toth LT, Cheng H, Edwards RL, Ashe E, Richey JN. 2017. Millennial-scale variability in the local radiocarbon reservoir age of south Florida during the Holocene. Quat. Geochronol. 42:130–143. doi: 10.1016/j.quageo.2017.07.005.

Völker C, Köhler P. 2013. Responses of ocean circulation and carbon cycle to changes in the position of the Southern Hemisphere westerlies at Last Glacial Maximum. Paleoceanography 28:726–739. doi: 10.1002/2013PA002556.

Waelbroeck C, Lougheed BC, Vazquez Riveiros N, Missiaen L, Pedro J, Dokken T, Hajdas I, Wacker L, Abbott P, Dumoulin J-P, et al. 2019. Consistently dated Atlantic sediment cores over the last 40 thousand years. Sci. Data 6:165. doi: 10.1038/s41597-019-0173-8.

Yu K, Hua Q, Zhao J, Hodge E, Fink D, Barbetti M. 2010. Holocene marine ^{14}C reservoir age variability: evidence from ^{230}Th-dated corals in the South China Sea. Paleoceanography 25. doi: 10.1029/2009PA001831.

Yu S-Y, Shen J, Colman SM. 2007. Modeling the radiocarbon reservoir effect in lacustrine systems. Radiocarbon 49:1241–1254. doi: 10.1017/S0033822200043150.

https://doi.org/10.1017/RDC.2022.66 Published online by Cambridge University Press